

Cyclostationarity and the cepstrum for operational modal analysis of MIMO systems—Part II: Obtaining scaled mode shapes through finite element model updating

D. Hanson^{a,*}, R.B. Randall^a, J. Antoni^b, T.P. Waters^c,
D.J. Thompson^c, R.A.J. Ford^a

^a*Mechanical and Manufacturing Engineering, The University of New South Wales, Kensington, NSW 2052, Australia*

^b*Laboratoire de Mécanique de Roberval, Université de Technologie de Compiègne, Compiègne 60205, France*

^c*The Institute of Sound and Vibration Research, University of Southampton, Southampton SO17 1BJ, UK*

Received 4 May 2006; received in revised form 30 November 2006; accepted 30 November 2006

Available online 18 January 2007

Abstract

This paper presents a new technique for scaling mode shapes, obtained from cepstrum-based operational modal analysis (OMA) techniques, such as that described in the companion paper, using finite element model updating. This OMA technique estimated frequency response functions (FRFs) between a cyclostationary input and response measurements. If the input is frequency white, the resulting FRFs can be obtained up to an overall scaling constant using the in-band poles and zeros identified in the OMA process and employing the response autospectrum as a reference to correct for the effect of out of band modes. In this way, the mode shapes would be scaled correctly relative to each other but would still have arbitrary overall magnitude. If the input is not white, then no reference is available to correct FRF regenerated from in-band poles and zeros, and so these FRFs will exhibit both an overall slope resulting from the effect of out-of-band poles and zeros, and an arbitrary magnitude. This overall slope will differ between measurement locations so even the relative scaling between the mode shapes will be lost. This paper describes a simple technique for recovering both the relative and overall scaling of the FRFs, and hence the mode shapes, based on finite element model updating.

© 2006 Elsevier Ltd. All rights reserved.

Keywords: Operational modal analysis; Scaled mode shapes; Cyclostationary; Cepstrum; Finite element model updating

1. Introduction

In recent years, there has been a great deal of research in the field of operational modal analysis (OMA). A number of techniques have been presented which aim to estimate the modal properties of a system, i.e. its resonances, damping and mode shapes, from response only measurements. The primary advantage of these techniques over traditional input/output modal analysis is that the in-service forces can be used to excite the

*Corresponding author. Tel.: +61 2 9385 6256; fax: +61 2 9663 1222.

E-mail address: david.hanson@student.unsw.edu.au (D. Hanson).

structure which avoids the need for an artificial input, such as a shaker or impact, and means that the modal properties recovered will be those that the system exhibits in service. These techniques include the frequency domain decomposition (FDD) algorithms [1,2], stochastic subspace iteration (SSI) [3,4] and the new PolyMAX technique [5]. However, all these techniques make an underlying assumption about the nature of the input—that it is frequency white.

One drawback of OMA is that, without knowledge of the input, both the overall and the relative scaling of the mode shapes is lost. Scaled mode shapes are important for a number of applications, including some forms of structural health monitoring and force identification [6,7]. If the input is frequency white then the relative scaling of a particular mode to all other modes is retained and only an overall scaling factor for all modes needs to be recovered in order to obtain scaled mode shapes. If the input is not white then both the relative and overall scaling is lost.

A number of OMA techniques have also emerged, which seek to exploit the properties of the cepstrum [8–10]. The cepstrum is a homomorphic operator, meaning that in the cepstrum domain the force and transfer function are additive. In addition, if the input is frequency smooth, then its cepstrum will be very short and so by removing the low “quefrequency” region (the name “quefrequency” is derived from “frequency” in the same way as “cepstrum” is derived from “spectrum”), the cepstrum of the transfer function can be isolated and curve-fitted to extract the system modal properties. This technique was originally developed for SIMO systems but has since been expanded to particular MIMO systems, one of which is described in the companion paper [11].

The ability to cope with non-white inputs and retain the relative scaling of the modes makes these techniques very powerful but they still require a priori knowledge in the form of an equalisation curve in order to overcome the effect on each transfer function of out-of-band modes. This a priori knowledge can take the form of a set of transfer functions from a traditional input/output modal analysis or a finite element model. However, as was discussed above, the advantage of OMA lies in the fact that input/output modal tests are not required, and finite element models are often poor predictors of the dynamic performance of a system. This paper presents a technique for obtaining the equalisation curves and scaling mode shapes by using an updated finite element model.

In the last few years, a significant amount of research has been devoted to the question of scaling mode shapes from OMA. One important contribution has been in obtaining scaling factors for each mode based on results of a separate, but significantly abridged, OMA in which the system has been modified, usually with a known added mass [12,13]. This technique has been shown to provide accurate mode shape scaling but is relatively expensive in that it requires a separate test and modifications to the system.

Often a relatively detailed FEA model exists even for complicated systems. It may not be suitable for dynamic analysis but so long as the mass distribution is relatively accurate, the stiffness can be coarsely updated using the resonances alone. The FRFs from the updated model can then be used to calculate the equalisation curves. Alternatively, a much simpler and coarser model can be used.

2. Theoretical overview

2.1. Equalisation curves

Gao and Randall [9,10] showed that, by isolating the region of the cepstrum, which is dominated by the transfer function, the system resonances and anti-resonances can be correctly identified. However, they also showed that this is not sufficient to reconstruct the FRF due to the influence of out-of-band modes which are excluded from the analysis. This could be corrected by estimating “phantom zeros”, artificially introduced in-band zeros, replacing out-of-band poles and zeros, which have no physical relation to the system, and generating a magnitude equalisation curve from these phantom zeros.

Rather than generating the equalisation curve from phantom zeros, subsequent developments of the cepstrum technique have included a far simpler difference method where the regenerated FRF is compared with a reference FRF, which may come from a previous measurement or a finite element model. The log

magnitude difference between the two is smoothed across the frequency range to provide the equalisation curve. The log magnitude difference is obtained from

$$\varepsilon(f_k) = \log |H_{\text{ref}}(f_k)| - \log |H_{\text{regen}}(f_k)|, \tag{1}$$

where H_{ref} and H_{regen} are the reference FRF and the FRF regenerated from in-band poles and zeros, respectively. The equalisation curve is then obtained by taking the Fourier transform of the difference to create a two sided “spectrum”

$$\Gamma(k) = \frac{1}{2N} \sum_{n=0}^{2N-1} \varepsilon(n) e^{-j\pi kn/N}, \tag{2}$$

where N is the length of ε . Taking the first μ samples of Γ , where μ is typically small (say ten), and applying a Hilbert transform relationship, the inverse Fourier transform is then employed to obtain the equalisation curve

$$H_{\text{eq}}(n) = \sum_{k=0}^{2N-1} \hat{\Gamma}(k) w_k e^{j2\pi kn/N}, \tag{3}$$

where $\hat{\Gamma}(1) = \Gamma(1)$, $\hat{\Gamma}(2 : \mu) = 2\Gamma(2 : \mu)$, and $\hat{\Gamma}(\mu + 1 : 2N) = 0$, and w_k is a smooth liftering function such as a half Hanning window. This process, including a typical equalisation curve, is represented in Fig. 1.

However, if significant differences exist between the resonance and anti-resonance locations in the regenerated and reference FRFs, if for example the finite element model used to generate the FRFs is inaccurate, then the equalisation curve can become distorted. This paper suggests first updating the finite element model using the resonances identified by an OMA technique which ensures that significant differences between regenerated and reference resonances and anti-resonances can be avoided. It should be noted however, and it is shown below, that the updated model need not be completely accurate.

2.2. Finite element model updating

Given that the OMA technique presented in the companion paper identifies both resonances and anti-resonances, it may be suggested that these could be used to obtain an accurate update of a finite element model [14–16]. The mode shapes from such a model would then be correctly scaled. However, as outlined in [17], the resonances alone may be sufficient to update a model in the frequency range of interest. This paper therefore pursues a different path, that of scaling the OMA FRFs using FRFs from a finite element model which has been updated using only the resonance information. The process described in this paper is summarised in Fig. 2.

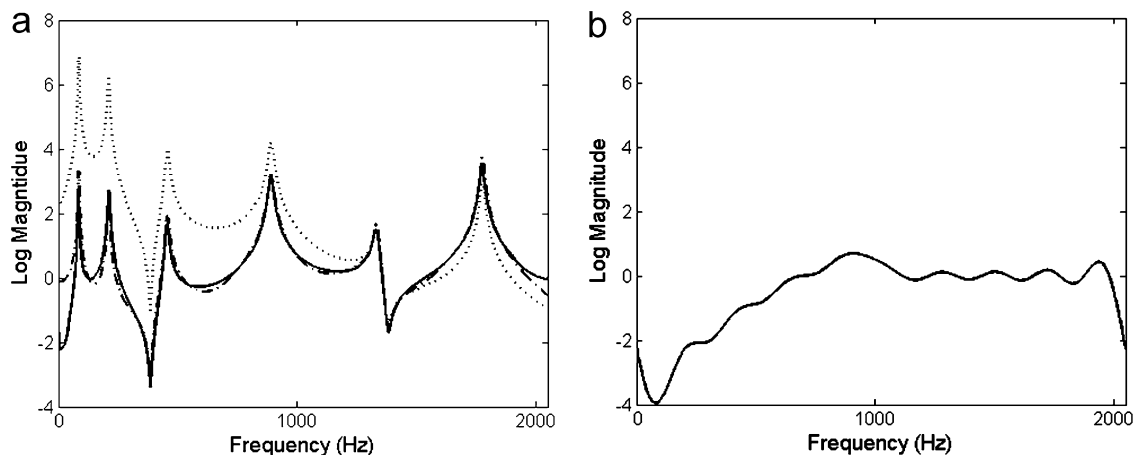


Fig. 1. Typical FRFs (a): reference (solid line), regenerated (.....) and scaled (-.-.-), and the corresponding equalisation curve (b).

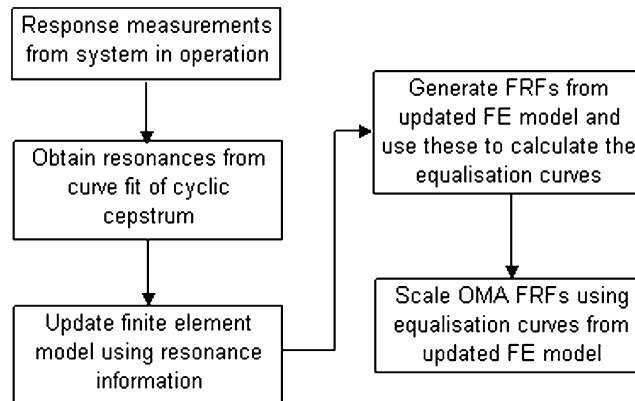


Fig. 2. Proposed procedure for obtaining scaled mode shapes from OMA.

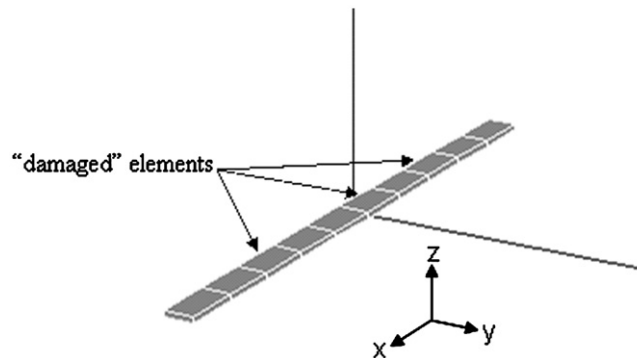


Fig. 3. Simulated beam.

3. Results

3.1. Simulation

The proposed technique was applied to a simulated system consisting of a free–free beam with localised damage, as represented in Fig. 3.

The beam was modelled using 10 identical brick elements with displacement dof only [18]. The use of brick elements may not provide the most accurate model for this system but it will be shown that the technique presented here is sufficiently robust that they are adequate for this application.

The density of steel was taken to be 7.85e3 kg/m³, and the elastic and shear moduli were 210e3 and 77e3 MPa, respectively. The mass and stiffness matrix of a typical element is given by

$$m = \frac{\rho h b l}{4} \begin{bmatrix} 1 & 0 & \dots & 0 \\ 0 & 1 & & \ddots \\ & & 2 & 0 & \vdots \\ \vdots & & 0 & 1 & \\ & \ddots & & & 1 & 0 \\ 0 & \dots & & & 0 & 2 \end{bmatrix}, \tag{4}$$

where ρ is the density and l, b, h are the length, breadth and height, respectively:

$$k = \begin{bmatrix} a_1 + 2a_3 & -a_1 + a_3 & a_4 & a_1 - 2a_3 & -a_1 - a_3 & -a_4 \\ -a_1 + a_3 & a_1 + 2a_3 & -a_4 & -a_1 - a_3 & a_1 - 2a_3 & a_4 \\ a_4 & -a_4 & a_2 & a_4 & -a_4 & -a_2 \\ a_1 - 2a_3 & -a_1 - a_3 & a_4 & a_1 + 2a_3 & -a_1 + a_3 & -a_4 \\ -a_1 - a_3 & a_1 - 2a_3 & -a_4 & -a_1 + a_3 & a_1 + 2a_3 & a_4 \\ -a_4 & a_4 & -a_2 & -a_4 & a_4 & a_2 \end{bmatrix}, \tag{5}$$

where $a_1 = Glb/4h, a_2 = Ghb/l, a_3 = Ehb/6l, a_4 = Gb/2, G$ is the shear modulus and E is the modulus of elasticity, and $u = \{ x_{1tx} \ x_{1bx} \ x_{1z} \ x_{2tx} \ x_{2bx} \ x_{2z} \}^T$ where x and z refer to displacements along the longitudinal axis of the beam and transverse to the longitudinal axis of the beam, respectively, and the subscripts t and b refer to the top and bottom of the beam.

The damage was simulated by a reduction in stiffness of three elements along the beam, akin to the cracks in the beam test rig experiment below, which produced a significant change in the resonances but only a minor change in the mode shapes of the beam, as represented in Table 1 and Fig. 4.

Table 1
Resonance frequencies of the modelled uniform and damaged beams

Bending mode	Resonance frequency (Hz)		% Difference
	Uniform beam	Damaged beam	
1st	103.39	83.100	20
2nd	282.22	211.60	25
3rd	553.06	453.65	18
4th	925.65	889.21	3.9
5th	1426.1	1331.7	6.6
6th	2108.5	1773.0	16

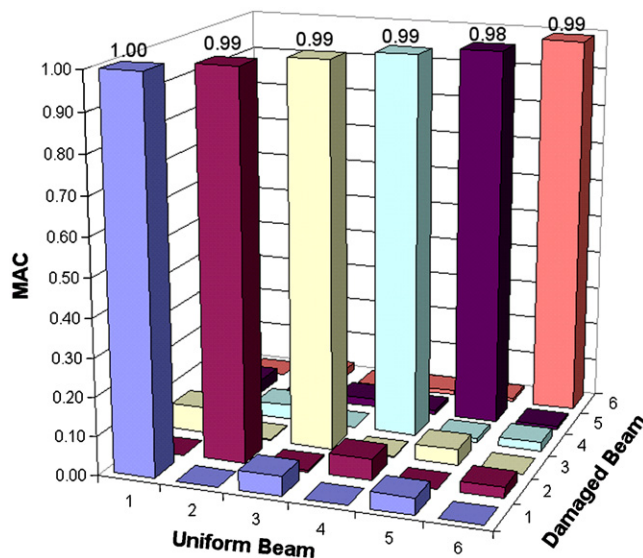


Fig. 4. MAC of bending modes 1–6 for the uniform and damaged beams.

3.2. Estimation of the system resonances

The responses of the simulated beam were calculated using a coloured cyclostationary excitation. This excitation was a burst random signal, with a duty cycle of 250 ms on/250 ms off, subsequently filtered using a first-order Butterworth low-pass filter. This provided a smooth but steep decay across the frequency range, ensuring that the scaling of the higher modes would be significantly distorted. Such distortion is experienced in many practical applications such as vibrations from internal combustion engines. The autospectrum of the input is represented in Fig. 5.

Noise free transfer functions were generated using a pole/residue model based on the resonances and mode shapes from the finite element model. These were used in conjunction with the cyclic spectra of the input to generate the cyclic spectra of the responses, which are represented in Fig. 6. As is clearly evident in this figure, the coloured input has severely distorted the magnitude of the modes across the frequency range so that both the relative and overall scaling of the modes has been lost.

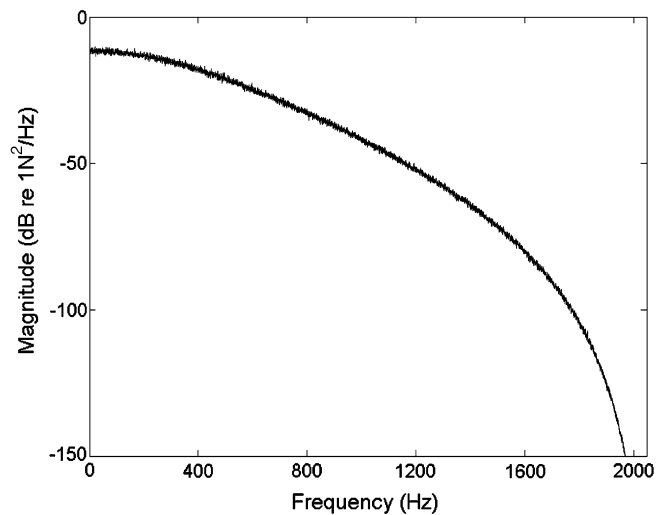


Fig. 5. Autospectrum of the coloured burst random excitation.

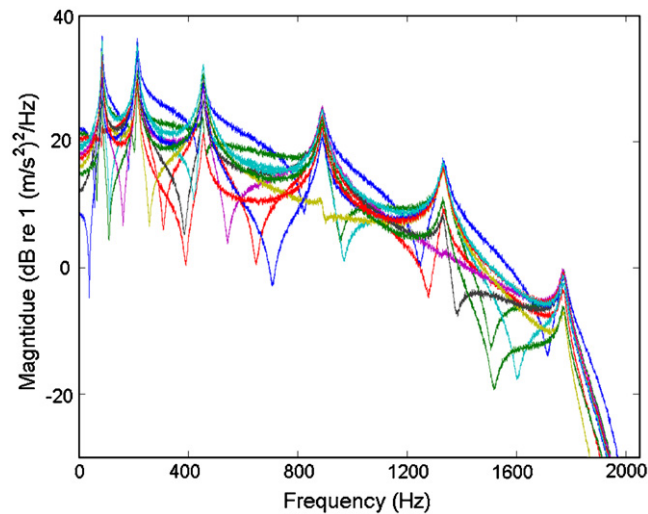


Fig. 6. Cyclic spectra of the responses of the simulated beam from each of the 11 measurement points.

The system resonances were then estimated using the OMA process described in the companion paper on the driving point cyclic spectrum. These resonances were then used to update the finite element model of the beam.

It should be emphasised that the OMA process employed here and described in the companion paper has no difficulty in identifying the system resonances and anti-resonances, even in the presence of such significant distortion. The only restriction is that the second-order cyclostationary component of the excitation is frequency smooth, which is far less restrictive than the usual white noise assumption.

3.3. Finite element model updating

The stiffness of the elements which exhibited damage were updated using a standard penalty function method [19] and the non-linear least squares optimisation algorithm in Matlab. The updated resonance frequencies are presented in Table 2.

3.4. Regeneration of the correctly scaled FRFs

The FRFs from the updated finite element model were then used in the generation of the equalisation curves, as described in Eqs. (1)–(3). These equalisation curves, together with the in-band poles and zeros identified during the OMA process described in the companion paper, were then used to regenerate the correctly scaled FRFs. The regenerated FRFs are presented in Fig. 7 below showing the effect of the equalisation.

Table 2
Updated resonance frequencies for bending modes 1–6

Bending mode	Resonance frequency (Hz)		% Difference
	Actual	Updated	
1st	83.10	83.04	0.07
2nd	211.6	211.55	0.02
3rd	453.65	453.90	0.06
4th	889.21	889.09	0.01
5th	1331.7	1331.8	0.01
6th	1773.0	1773.1	0.01

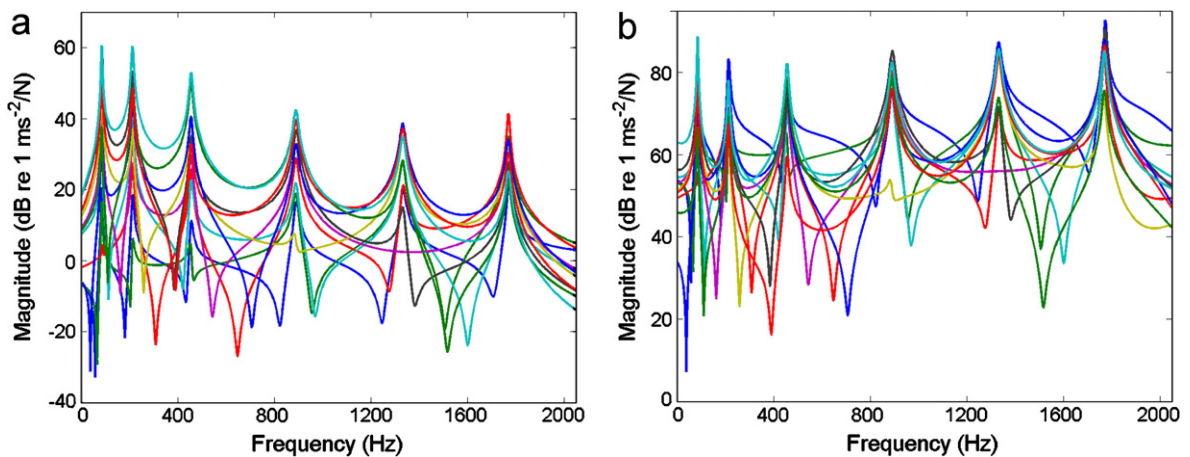


Fig. 7. Regenerated FRFs of the simulated beam from the OMA process—without equalisation (a) and with equalisation (b).

It is important to emphasise that the equalisation does not counteract the distortion of the coloured inputs, rather it merely accounts for the effect of the out-of-band modes. By separating the input and transfer function in the cepstrum domain, the estimated system properties are completely unaffected by the colour of the input. This robustness to non-white inputs is one advantage of cepstrum based system identification techniques.

The scaled mode shapes are compared with those of the “damaged” beam finite element model in Fig. 8.

The correlation of the mode shapes is further emphasised by the modal assurance criterion (MAC), as represented in Fig. 9.

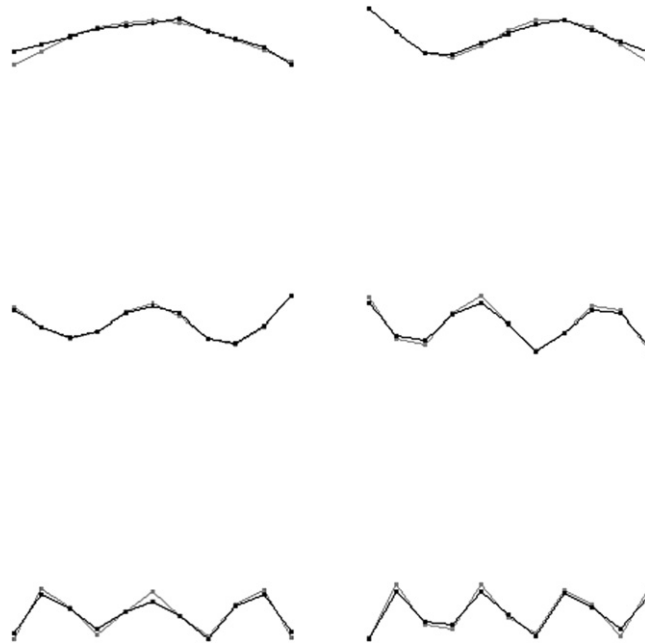


Fig. 8. Bending mode shapes 1–6 of the simulated beam—from FE model (grey) and from the OMA process after scaling (black).

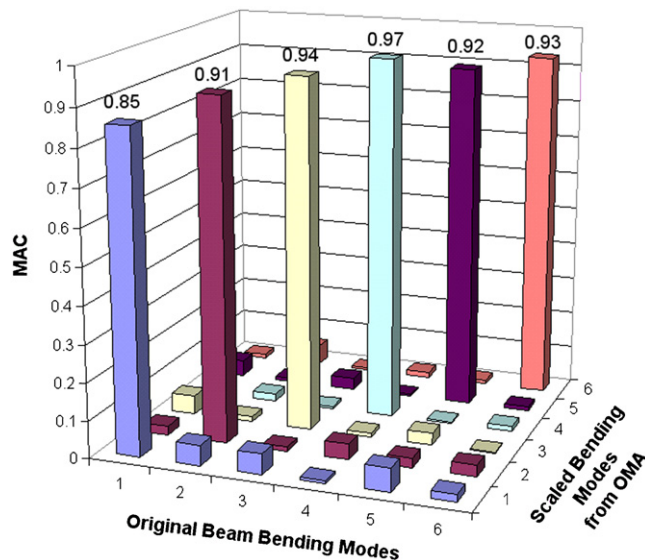


Fig. 9. MAC of the scaled mode shapes from OMA and from the original beam model.

Although the MAC does not take into account the scaling of the modes, this figure shows that the equalisation of the FRFs was successful as the unequalised FRFs each have a unique slope, which distorts each dof independently across the frequency range, as seen in Fig. 7. As a result any mode shape information is severely affected and the MAC would be greatly reduced, as represented in Fig. 10.

4. Experimental results

4.1. Experiment set-up

The technique was tested using measurements taken on a steel beam test rig, represented in Fig. 11. The beam was identical to the simulated beam used in the previous section, with dimensions $20 \times 50 \times 1000 \text{ mm}^3$, was suspended on soft springs to simulate a free–free support with the highest rigid-body mode at 5 Hz (pitching mode), well separated from the first bending mode at 95 Hz.

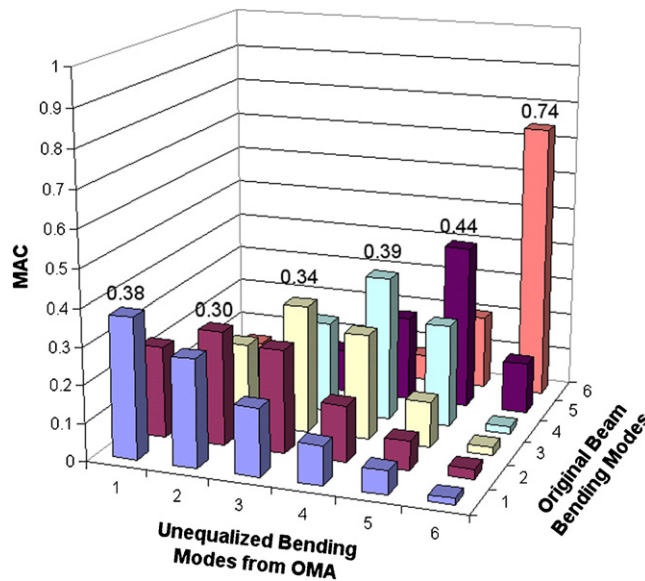


Fig. 10. MAC of the mode shapes from the unequalised FRFs from the OMA process and from the original beam model.

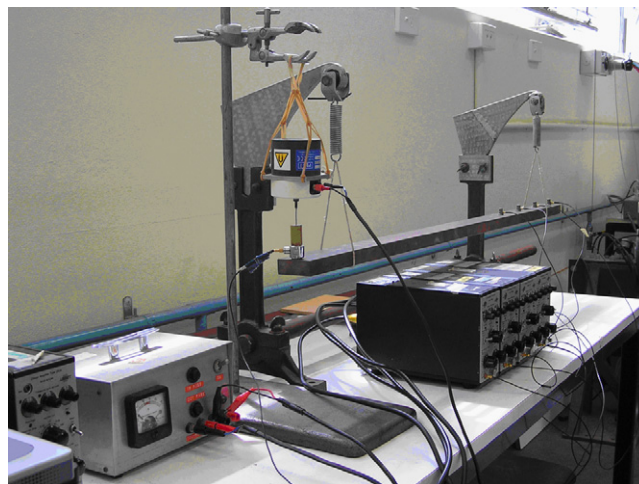


Fig. 11. Steel beam test rig.

The beam has two cuts across its width and through approximately 75% of its depth located at 190 and 540 mm from the left-hand edge. The beam was excited through a shaker mounted on the longitudinal centreline of the beam at the left hand edge. The responses to this excitation were measured at 11 equally spaced locations along the beam, also along its centreline. Exciting along the centreline of the beam ensured only the bending modes were excited which allowed a simplified finite element model to be employed.

The excitation consisted of burst random noise, with 250 ms on/250 ms off duty cycle, across a frequency range of 2048 Hz. The noise was coloured using a pink filter creating a significant scaling distortion of the response spectra. The response measurements were sampled at 4096 Hz and each measurement was of 10 min duration. The long measurement length was required in order to allow sufficient averaging to achieve a smooth cyclic spectrum.

The input autospectrum, as measured by the force transducer, of a typical measurement is represented in Fig. 12.

Evident in this figure is the overall shape of the pink filter, the effect of the anti-aliasing filter above 1.6 kHz and the peak notches at each resonance. These peak notches are due to the separation between the natural frequency of the beam itself (as registered by the ratio of response to measured force) and the maximum response at the natural frequency of the beam plus shaker moving element. In OMA, this is generally not encountered because the system is excited by in-service forces and not through an attached system such as a shaker.

The cyclic spectra were calculated in the manner described in the companion paper. The eleven cyclic spectra are represented in Fig. 13.

The distortion due to the coloured input is especially evident when the cyclic spectra are compared with the corresponding FRFs, as represented in Fig. 14 for a typical measurement.

The effect of this distortion is to corrupt the relative scaling of each mode, meaning that each mode now has an independent and arbitrary scaling. If the input was white, then only an overall scaling for all modes would need to be recovered.

4.2. Finite element model

The beam was modelled using 20 identical brick elements with displacement dof only, as described above. The material properties were identical to those used in the simulation above.

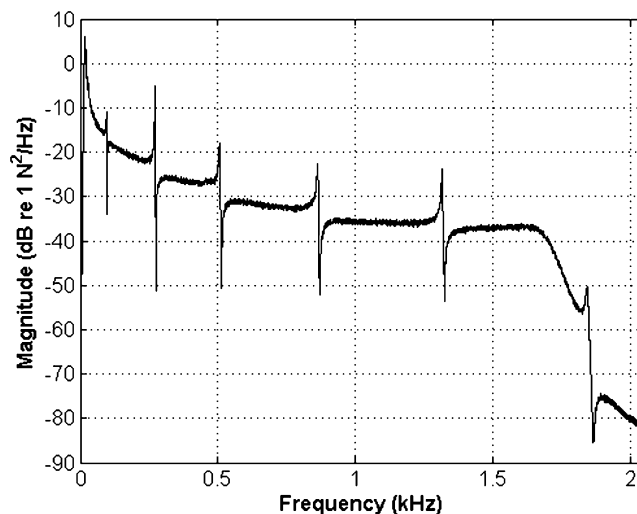


Fig. 12. Typical measured input autospectrum of the beam.

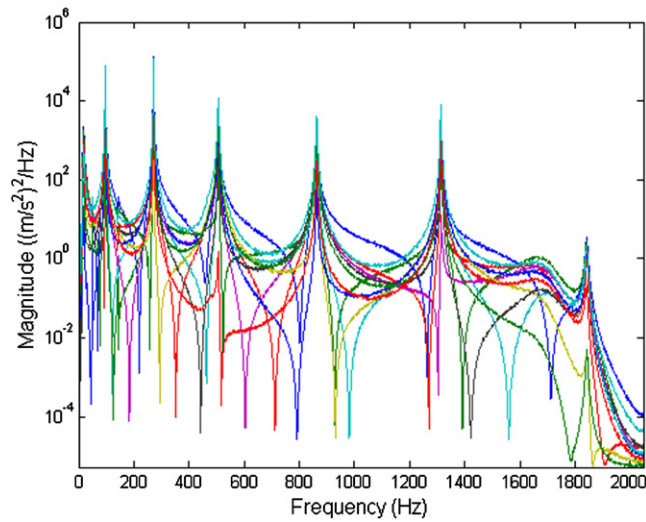
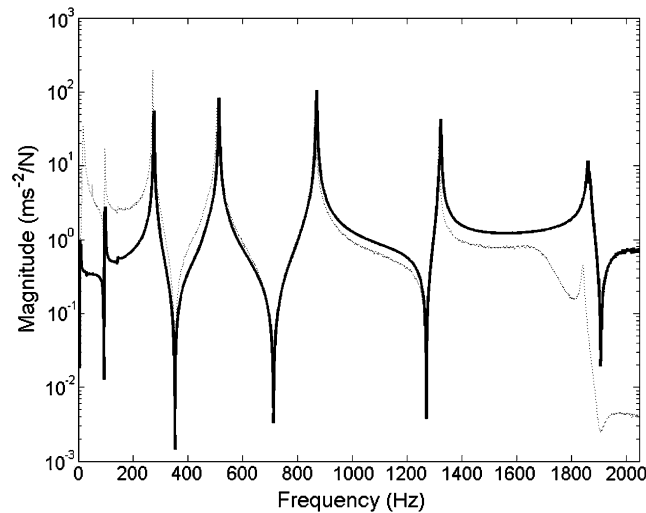
Fig. 13. Cyclic spectra of the beam for $\alpha = 1/T$.

Fig. 14. Comparison of a typical FRF (solid line) and the corresponding cyclic spectrum (dashed line) which has been distorted by the coloured input.

4.3. Finite element model updating

The resonance frequencies in the range 1–2048 Hz were estimated from one of the cyclic spectra above by curve-fitting in the cepstrum domain. These resonance frequencies were then used to update the finite element model to account for the effect of the cuts.

The effect of the cuts was represented in the model as reduced values of the elastic modulus in the corresponding elements. The elastic modulus of these two elements was then updated using the non-linear least squares optimisation algorithm in Matlab. The updated elastic moduli were 85.5 and 66.7 MPa, respectively. The resonances of the original and updated model and those estimated from the test rig are contained in Table 3.

Table 3
Resonances of the steel beam test rig and updated finite element model

Bending mode	Resonance frequency (Hz)			% Error in FE model	
	Original FE model	Updated FE model	Test rig	Before updating	After updating
1 st	106.6	93.63	95.50	12	2.0
2nd	292.3	278.3	275.0	6.3	1.2
3rd	570.2	499.5	512.0	11	2.4
4th	938.8	868.3	869.0	8.0	0.12
5th	1398	1290	1320	5.9	2.3
6th	1948	1911	1860	4.7	2.7

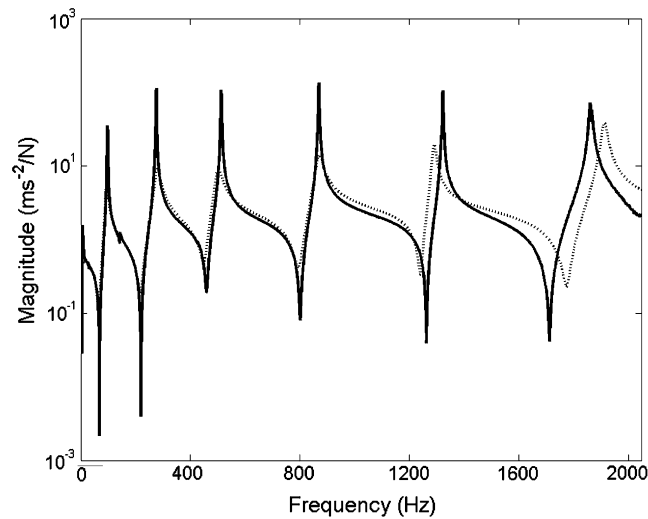


Fig. 15. Comparison of the driving point FRF from measurement (solid line) and from the updated finite element model (dashed line).

As can be seen above, the resonance-only update improves the accuracy of the modelled resonances, but some significant error still exists. This can be seen in a comparison of a typical FRF from the updated model and the measurements from the beam, as represented in Fig. 15.

FRFs from this updated model were then used to calculate the equalisation curves in the OMA process. The driving point FRF and a typical transfer FRF are represented in Fig. 16.

It is important to note that this process was robust to the small errors still present in the updated FRFs, both in terms of frequency and damping as can be seen in Fig. 15, indicating that the relatively coarse model and resonance-only update were sufficient to generate the equalisation curves. In addition, the resonances of the scaled FRFs from OMA can be seen to be slightly lower than those of the measured frequency response functions. As mentioned above, this is due to the added mass of the shaker moving element, which affects the response spectra but not the frequency response functions. This effect would be observed in any OMA process which uses response spectra as its basis.

Interestingly, the effect of out-of-band modes in the pole/zero model employed here is much less in driving point measurements than on transfer measurements; the opposite of the traditional pole/residue model. As Gao and Randall [9] explain, the amplitude ratio of a out-of-band poles and zeros tend to balance in driving point measurements because there are an equal number of out-of-band poles and zeros. Therefore, the in-band effect is very small. This is not the case in transfer measurements, which exhibit more poles than zeros and so their amplitude ratio is unbalanced. The equalisation curves of driving point measurements therefore will be relatively flat and those of transfer measurements will be relatively steep.

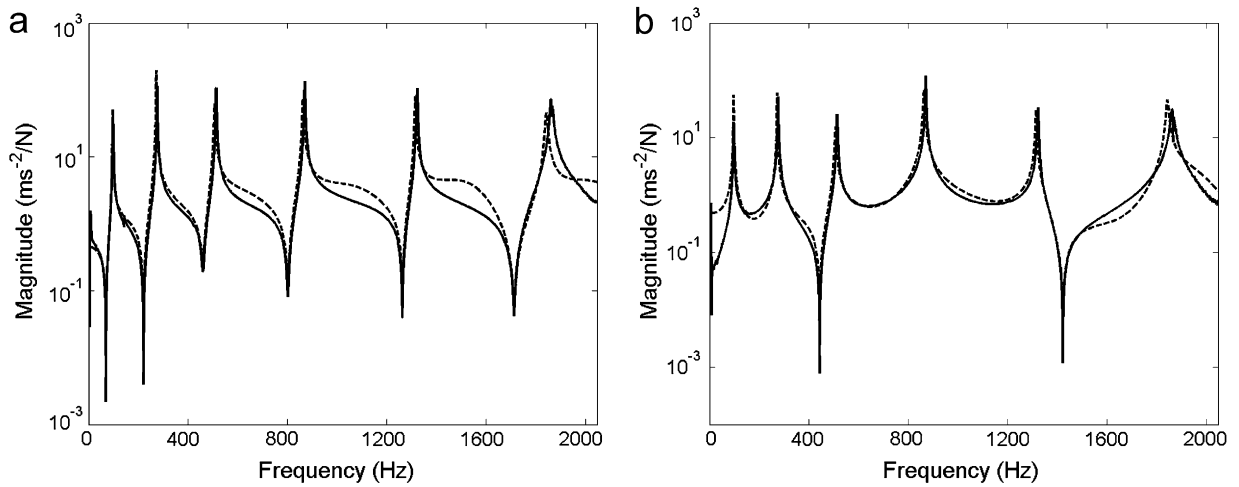


Fig. 16. Comparison of correctly scaled FRFs from OMA (dashed line) and measured (solid line); driving point (a) and typical transfer (b).

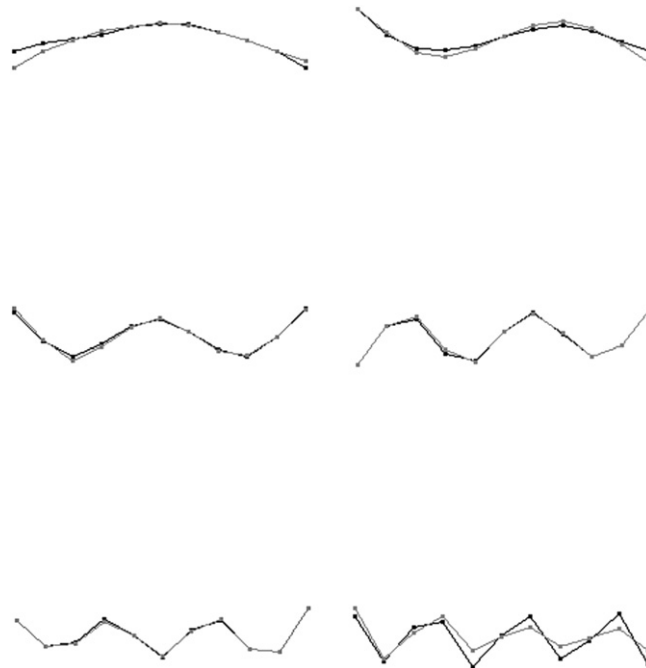


Fig. 17. Comparison of scaled mode shapes from OMA (black) and from input/output modal analysis (grey).

4.4. Correctly scaled mode shapes from OMA

The correctly scaled FRFs were curve-fitted using commercial software and the mode shapes generated. These mode shapes are compared with those from the measured FRFs in Fig. 17. As can be seen, the scaled mode shapes from the OMA process compare relatively well with those from the traditional input/output modal analysis.

The mode shapes in Fig. 17 may be also be compared using the MAC as represented in Fig. 18 although as discussed above, this does not provide a measure of scaling of the modes and so represents the degree to which the equalisation was successful.

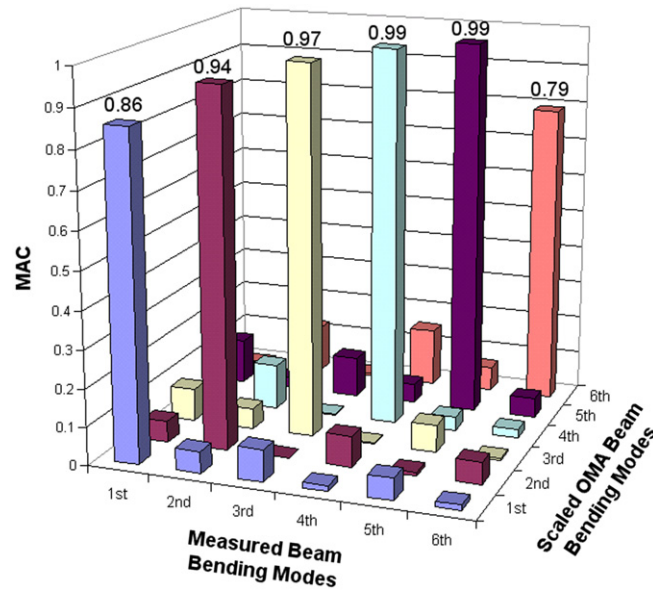


Fig. 18. MAC of the mode shapes from OMA and from input/output modal analysis.

5. Discussion

This paper presented a simple method for recovering both the relative scaling between modes, and the overall scaling of all modes, which are lost in OMA when the input excitation is not white. The technique involved identifying the resonances from a single distorted response spectrum and using these to update a simple finite element model. The frequency response functions from this updated model could then be used to provide the equalisation curves for a cepstrum based blind identification technique.

The technique was demonstrated on a simulated beam with localised damage and using measurements taken on a steel beam test rig which had localised damage in the form of cuts across its width. In both cases, the input excitation decayed significantly across the frequency range so that both the relative and overall scaling of the modes was lost. The technique was shown to recover scaled mode shapes in both cases, even when small differences existed between the FRFs of the updated model and the response cyclic spectra.

This technique is proposed in conjunction with a cyclostationary and cepstrum based OMA technique outlined in the companion paper which may be applied to vehicles with internal combustion engines. In this way, it might be possible to obtain scaled mode shapes of vehicles such as locomotives and passenger trains from in-service measurements.

Acknowledgements

The authors would like to thank Mr. Russell Overhall for his assistance with the experimental phase of this paper and Dr. Hiro Endo for his editorial advice. This research was funded by The Australian Research Council and The Defence Science and Technology Organisation under the Centre of Expertise Scheme.

References

- [1] R. Brincker, L. Zhang, P. Andersen, Output-only modal analysis by frequency domain decomposition, in: Proceedings of The ISMA25 Noise and Vibration Engineering, Leuven, Belgium, 2000.
- [2] R. Brincker, L. Zhang, P. Andersen, Modal identification from ambient responses using frequency domain decomposition, in: Proceedings of the 18th International Modal Analysis Conference, San Antonio, TX, 2000.

- [3] B. Peeters, G.d. Roeck, Reference-based stochastic subspace identification for output-only modal analysis, *Mechanical Systems and Signal Processing* 13 (6) (1999) 855–878.
- [4] B. Peeters, G.d. Roeck, Stochastic system identification for operational modal analysis: a review, *Journal of Dynamic Systems, Measurement and Control* 123 (2001) 659–667.
- [5] B. Peeters, H.V.d. Auweraer, Polymax: a revolution in operational modal analysis, *First International Operational Modal Analysis Conference*, Copenhagen, 2005.
- [6] E. Parloo, et al., Increased reliability of reference-based damage identification techniques by using output-only data, *Journal of Sound and Vibration* 270 (4–5) (2004) 813–832.
- [7] E. Parloo, et al., Force identification by means of in-operation modal models, *Journal of Sound and Vibration* 262 (2003) 161–173.
- [8] R.B. Randall, Y. Gao, Extraction of modal parameters from the response power cepstrum, *Journal of Sound and Vibration* 176 (2) (1994) 179–193.
- [9] Y. Gao, R.B. Randall, Determination of frequency response functions from response measurements—II: regeneration of frequency response functions from poles and zeros, *Mechanical Systems and Signal Processing* 10 (3) (1996) 319–340.
- [10] Y. Gao, R.B. Randall, Determination of frequency response functions from response measurements—I. Extraction of poles and zeros from response cepstra, *Mechanical Systems and Signal Processing* 10 (3) (1996) 293–317.
- [11] Hanson, D., et al., Cyclostationarity and the cepstrum for operational modal analysis of MIMO systems—Part I: modal parameter estimation, *Mechanical Systems and Signal Processing* (2007), doi:10.1016/j.ymssp.2006.11.008.
- [12] E. Parloo, et al., Sensitivity-based operational mode shape normalisation: application to a bridge, *Mechanical Systems and Signal Processing* 19 (2005) 43–55.
- [13] E. Parloo, et al., Sensitivity-based mode shape normalisation, *Mechanical Systems and Signal Processing* 16 (5) (2002) 757–767.
- [14] W. D’Ambrogio, A. Fregolent, Results obtained by minimising natural frequency and antiresonance errors of a beam model, *Mechanical Systems and Signal Processing* 17 (1) (2003) 29–37.
- [15] W. D’Ambrogio, A. Fregolent, The use of antiresonances for robust model updating, *Journal of Sound and Vibration* 236 (2) (2000) 227–243.
- [16] K. Jones, J. Turcotte, Finite element model updating using antiresonant frequencies, *Journal of Sound and Vibration* 252 (4) (2002) 717–727.
- [17] D. Hanson, et al., The role of anti-resonances from operational modal analysis in finite element model updating, *Mechanical Systems and Signal Processing* 21 (1) (2007) 74–97.
- [18] Y.W. Kwon, H. Bang, *The Finite Element Method Using Matlab*, second ed, CRC Press, Boca Raton, FL, 2000.
- [19] M.I. Friswell, J.E. Mottershead, *Finite Element Model Updating in Structural Dynamics*, Kluwer Academic Publishers, London, 1999.